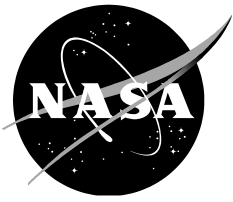


NASA Aeronautics Research Institute (NARI) 2013 Phase I



Innovative, Low-cost Phased Microphone Array Design for Moderate-Scale Aeroacoustics Tests

*W. Clifton Horne and Nathan J. Burnside
Ames Research Center, Moffett Field, California*

National Aeronautics and
Space Administration

*Ames Research Center
Moffett Field, CA*

July, 2014

Acknowledgments

This research was funded by NASA Aeronautics and Mission Directorate (ARMD) NASA Aeronautics Research Institute (NARI) Round 2 Phase 1 Seedling Fund. Additional resources were provided by ARMD Fixed Wing Project to build additional sensors and support acquisition of acoustic data during the NASA/Boeing sweeping-jet active flow control rudder experiment. Cooperation and accommodation from the aerodynamic test teams from NASA Environmentally Responsible Aviation (ERA) Program, Boeing, and the Arnold Engineering Development Center(AEDC) National Full-Scale Aerodynamics Complex (NFAC) is also gratefully acknowledged. Substantial portions of the array mechanical and electronic systems were designed by Aerospace Computing Incorporated (ACI), and advice and recommendations regarding array processing were provided by Optinav, Inc.

NARI: Michael Dudley, Koushik Datta, ARMD Fixed Wing Project: Ruben Del Rosario, NASA Ames Research Center: Robert Fong, Kevin James, Ed Schairer, NASA Langley Research Center (ERA program) Tony Washburn, John Lin, Robert Mosher, Boeing: Ed Whalen, AEDC NFAC Charles Rogers, Arturo Zamora, Aerospace Computing, Inc.: Hiro Kumagai, Optinav: Robert Dougherty

This report is available in electronic form at
<http://nari.arc.nasa.gov>

NOMENCLATURE

c	sound speed
CSM	array microphone cross spectral matrix
D	diameter of array pattern
$\Delta\theta$	angular resolution of array
θ	emission angle of source, $\theta = 0$ for emission upstream
f	frequency, Hz
f_{RL}	frequency of Rayleigh resolution limit
M	Mach number, U_0/a
p	acoustic pressure rms level, Pa
p_{REF}	acoustic reference rms level, 20×10^{-6} Pa
U_C	convection speed of boundary layer disturbances
U_0	free stream velocity
x	distance from origin in the streamwise direction
y	distance from the array plate in the direction normal to the plate

Low-cost Phased Microphone Array Design for Moderate-Scale Aeroacoustics Tests

W, Clifton Horne, Nathan J. Burnside, Ames Research Center

Summary

A new wall mounted array was designed, assembled, calibrated and tested to 300 kt ($M=0.45$) in the acoustically treated AEDC NFAC 40- by 80-Ft Wind Tunnel at NASA Ames Research Center to characterize reductions in background noise achieved with porous wind screens and advanced array processing methods. Two configurations were evaluated: 24 electret microphones in a spiral pattern within a 32 inch diameter circle on a solid plate flush with the flow, and the same pattern on a plate recessed $\frac{1}{2}$ " behind a Kevlar windscreen that was flush with the flow. The latter demonstrated background noise reductions of 15-25 dB (1/3 octave spectra levels) relative to an in-flow microphone with a quiet nosecone, while the former demonstrated reductions that were less pronounced. The arrays demonstrated useful measurement of peak and spatially integrated levels of low intensity sources typical of new quiet vehicle configurations over a bandwidth of 160 to 20,000 Hz.

Four additional arrays with windscreens were built, calibrated, and installed in the wind tunnel for acoustic measurements of a flight-hardware Boeing 757 rudder equipped with sweeping jet active flow control to increase the maximum control effect available during an engine-out emergency. These measurements were the first acoustic characterization of this configuration at any scale, and will be used to help plan a flight-demonstration of the concept in the near future. Although the arrays were designed for accurate level measurement rather than high-resolution source location, the arrays were able to discriminate individual control actuators at high frequencies.

The new in-flow array design enabled accurate acoustic level measurements in the presence of high background noise at low relative cost by using a small array size with low sensor count, similar to the Small Aperture Directional Array (SADA) introduced by Humphreys and Brooks. This concept enabled further improvements in test productivity and reduced test costs and schedule impacts by deploying multiple fixed arrays rather than a single traversing array. This approach will allow meaningful acoustic measurements in test programs that would otherwise forgo them due to budget and schedule constraints.

1. Introduction

1.1 Background: Phased microphone arrays in wind-tunnel aeroacoustic research

For many decades, the noise generated by aircraft during landing and take-off operations has been regulated by local and federal agencies to remain within limits that have been and will continue to be progressively restrictive. The need to understand and

further reduce aircraft noise has motivated the introduction of new diagnostic and predictive technologies that identify and characterize flight vehicle noise sources that may be reduced in level or eliminated with improved design in order to satisfy increasingly stringent aircraft noise rules.

The phased microphone acoustic source location array was applied to aeroacoustic research in the mid 1990's as an improvement over single omnidirectional microphones and elliptical reflector directional microphones then in use.¹ The phased microphone array usually consists of either a linear, planar, or non-planar distribution of microphones exposed to the acoustic source field of interest. The direction of a source or distribution of sources can be estimated by measuring the time delay or phase shift of signals between the microphones.

If the source location is known, the associated acoustic level at the array can be determined by applying the appropriate time delays for each microphone and summing the signals, termed conventional delay-and-sum time-domain beamforming. The level measured by the array will correspond to the level sensed by a single microphone, but has the benefit of reduced sensitivity to other sources that are not of interest, including facility background noise. Alternatively, the Fourier transform of each microphone signal can be phase-shifted by the appropriate amount and summed (frequency-domain beamforming).

More generally, the source locations are not known at the time of measurement, and a regular grid of potential source locations is "scanned" for source locations and level distributions at different frequencies. The scanned results can then be assembled to form a visual acoustic image of the source field superposed on a corresponding optical image at each frequency band of interest. This composite image can then be spatially integrated to generate an overall source level, or integrated over smaller subregions to estimate levels of various noise components. For wind tunnel applications, the analysis process, including effects of convection, was described by Mosher.²

Placements of arrays that have been used successfully in recent tests are depicted in Fig.1, which shows a notional aeroacoustic test set-up in an open-jet wind tunnel with a solid floor. An array may be placed outside the flow on either side or above the model, for which sound waves emanating from the model must propagate through the unsteady turbulent free-shear layer. Arrays may also be positioned in the floor underneath the turbulent wall/floor boundary layer, or in a fairing supported on a strut to position the array above the boundary layer. In the latter case, the array will be underneath the fairing turbulent boundary layer that is usually much thinner than the wall/floor boundary layer or free-jet shear layer. The arrays shown on the floor can also be used on the walls and ceiling of a fully enclosed hard-wall or acoustically treated wind tunnel. In each case, the turbulent shear- or wall-boundary layer will modify the waves originating from the source of interest and need to be accounted to accurately estimate levels from the array system.

Some recent examples of aeroacoustic test set-ups with microphone arrays are shown in Fig. 2. Fig. 2a shows the traversable Medium Aperture Directional Array (MADA) array outside of the flow of the NASA Langley Research Center (LaRC) Quiet Flow Facility (QFF) for measurement of the acoustic field of a scaled landing gear.³ Fig. 2b shows a similar traversable large array above the upper free shear layer of the NASA

LaRC 14- by 22-Foot wind tunnel for measurement of the acoustic field of an inverted Hybrid Wind-Body (HWB)⁴ configuration. Fig. 2c shows a wall-mounted array in the NASA ARC 12-ft Pressurized Wind Tunnel for measurement of a semi-span MD-11 aircraft.⁵ Finally, Fig. 2d shows (to the far left) an in-flow strut-mounted array in a streamlined fairing for measurements of the acoustic field of a sting-mounted Cruise Efficient Short Take-Off and Landing (CESTOL) model with trailing- and leading-edge continuous slot blowing^{6,7} that were obtained in the AEDC NFAC 40- by 80-ft Wind Tunnel at NASA Ames Research Center (ARC). Also shown in Fig. 2d is a line of seven strut-mounted single microphones with streamlined nosecones.

Calibration of the 48 inch diameter, 48 element in-flow array and strut mounted microphones used in the CESTOL test referenced above was conducted after that study. During this calibration, empty-tunnel background noise was measured up to $M = 0.4$, and response to an in-flow speaker was measured up to $M = 0.3$, similar to the calibration of the present study. A sample hemispheric conventional beamform scan from this test at 100 kts ($M=0.15$) for the 800 Hz 1/3 octave band is shown in Fig. 3. At this frequency, the dominant background noise sources are the tunnel drive noise from upstream and downstream, as well as strut noise from the in-flow microphones. With array processing, these sources may be suppressed by 10-20 dB by using array-processing methods to be described in the following sections.

1.2 Phased microphone array configurations: resolution, errors, uncertainties, signal-to-noise, and practical limitations.

Resolution

The primary benefits of using phased microphone arrays for aeroacoustics research are: 1) determining the locations and levels of noise sources associated with the target source of interest and 2) rejecting interfering sources of noise unrelated to the target source (e.g. facility drive noise, noise from model and sensor support struts in the flow, and turbulent hydrodynamic noise from boundary layers over wall-mounted or strut-mounted in-flow sensors) in order to obtain accurate source level measurements.

For a phased microphone array with microphones placed on a plane within a circular aperture of diameter D and processing with conventional delay-and-sum beamforming, two sources $\Delta\theta$ apart can be seen as separate sources down to a low limit frequency f_{RL} :

$$f_{RL} = 1.22 c / (\Delta\theta * D) \text{ radians, or}$$

$$f_{RL} = 70 c / (\Delta\theta * D) \text{ degrees}$$

This is the Raleigh resolution limit for conventional delay-and-sum beamforming. For example; an array pattern 32 inches (81 cm) in diameter at 2000 Hz can resolve two sources about 15° apart with conventional beamforming. Below this frequency the array becomes less effective for target source location, but retains the ability to suppress interfering background noise, and the spatial integral of the hemispheric map still compares well with the level sensed by an omni-directional microphone, as will be discussed later in this report.

The high frequency limit of a particular array is encountered at wavelengths too small for the wave pattern to be adequately sampled by the microphones on the array. Post-processing of the conventional beamform result with methods such as DAMAS⁸, TIDY,⁹

and others can provide useful resolution at frequencies lower than the Rayleigh criterion. These and more recent methods such as Functional Beamforming¹⁰ can also suppress sidelobe artifacts in the array point-spread function that limit the dynamic range particularly near the high-frequency limit of the array. If the frequency range of interest is larger than practical to achieve with a single array pattern, then a number of differently sized arrays can be nested with the potential benefit of reducing total microphone count by eliminating duplicate microphone positions. For example, the recent airframe noise study of the HWB configuration at Boeing's Low-Speed Aeroacoustic Facility (LSAF) open-jet tunnel used four nested arrays with the largest array of 170 microphones in a 126 in x 95.6 inch aperture, and the smallest array of 170 microphones in a 12 x 9 inch aperture.¹¹

Errors related to array size

The microphone array captures radiated noise over a finite solid angle rather than a single point as is the case for a single microphone. At least two errors can result from this. First, if the source radiation pattern is highly directional, the array processing will generate a level estimate that is an average over the array microphones if the source is assumed to be omnidirectional. Second, if the source is a distribution of uncorrelated or weakly correlated sources, then the coherence of the acoustic signals between each microphone pair may be reduced for higher frequencies and larger sensor separation distances within the array, resulting in estimated source levels less than the level measured at a point. Panda¹² discusses modification of the array processing method based on measured coherence between microphones to correct for loss of spatial coherence with a finite array for distributed sources such as jet and rocket plumes. The de-correlation effect is also encountered if the acoustic waves from the target source traverse a shear- or boundary-layer prior to sampling by the array microphones, as reported by Dougherty¹³ and Pires.¹⁴

Errors related to array aperture size may be reduced by using smaller arrays at the expense of spatial resolution. The Small Aperture Directional Array (SADA)¹⁵ and the Medium Aperture Directional Array (MADA)³ were developed at LaRC to maximize level measurement accuracies by minimizing array capture angle and using array directional response to exclude known interfering sources such as the sidewalls of an open jet facility such as the QFF. A major component of the present study consists of adapting the SADA-type level-sensing array to operate as a wall-mounted array in a closed wind tunnel, with some design and operational differences.

Other errors and uncertainties can result from differences in microphone amplitude and phase response, geometry of the array, and distortions in the propagation path such as through sheared or turbulent layers surrounding the target source and at the wind tunnel stream boundaries. Underbrink¹⁶ lists many of the factors that can degrade measurement accuracy and recommended methods of reducing response uncertainty, as well as options for array pattern design. As previously noted, Dougherty¹³ and Pires et al.¹⁴ examined the effects of wave propagation through boundary- and shear-layers and found strongly increasing decorrelation of the acoustic signal as functions of frequency, microphone spacing, and boundary layer thickness.

Acoustic radiation from sources other than the target source can limit dynamic range and degrade measurement accuracy with both in-flow and out-of-flow array configurations.

These sources include facility drive noise and noise from turbulent or separated flow interacting with support struts and other tunnel hardware. Humphreys, et al.¹⁷, Blacodon¹⁸, and others^{19, 20} describe methods for effectively subtracting interfering noise sources. One such method is to directly subtract the cross-spectral-matrix (CSM) of wind tunnel noise without the target source from the CSM that includes the target source and same background noise sources before processing. The effectiveness of this method will be examined in this report.

Experimental aeroacoustics research often has the goal of characterizing the target source far-field noise over a wide range of frequencies, directions, test conditions, and parametric configuration changes. With a single or small number of arrays, as used in many programs to date, this involves traversing the array(s) or microphones through the directional field for each configuration of interest. This may be the only practical approach for test programs for which characterization of the full acoustic field is of primary interest, and aerodynamic characterization is important but secondary. In this circumstance, high-fidelity aerodynamic data is usually obtained in a separate test entry with well-defined hard-wall bounding conditions comparable to corresponding numerical simulations.

It is also of interest to develop the capability to obtain preliminary but meaningful acoustic measurements in test programs where aerodynamic data is of primary interest. In these programs, acoustic measurements need to be acquired on a non-interference basis regarding sampling durations and acoustic sensor intrusion. In this case substantial coverage of the directional acoustic field with multiple fixed arrays may be preferable to traversing array(s) to maintain aerodynamic test productivity goals.

Factors affecting aeroacoustic research using wall/floor-mounted arrays and strut-mounted in-flow arrays

Wall-, floor-, or strut-mounted arrays provide acoustic measurement access within a closed test section or from the floor of a partially open jet facility as shown in Fig. 1. The array(s) may be fixed to the wall and subjected to the unsteady turbulent wall boundary layer, or mounted within a fairing on a fixed or traversing strut above the wall/floor boundary and subjected to the thinner turbulent boundary layer over the fairing. Either case results in background noise sources different than with the out-of-flow array generally used in the open-jet or acoustically-transparent lined facilities, and methods have been developed to reduce the levels of these noise sources.

Array processing methods based on the time-averaged cross-spectral matrix suppress local boundary layer pressure fluctuations since these noise components are either weakly correlated across most of the microphone pairs, or are correlated for convection speeds less than the sound speed. The boundary layer pressure fluctuations may also be suppressed 15-20 dB by recessing the array microphone plate behind an acoustically transparent screen such as Kevlar^{21, 22} or wire cloth.²³ The subsonically convecting pressure disturbances decay exponentially with recess depth as predicted by a wavy-wall analogy as :

$$20\log_{10}(p/p_{REF}) = -4.3(4\pi fy)/U_C,$$

where f is the frequency, y is the recess depth, and U_C is the convection speed of turbulence. For example, the attenuation is approximately 19 dB at 100 kts and 1000 Hz for a recess of 0.5 inches, assuming a convection speed 70% of freestream speed U_0 . Although stronger attenuations are predicted for higher frequencies, other sources such as secondary noise from turbulence interacting with the wind screen can limit the effectiveness of this approach unless further optimization of the windscreen or microphone mount design is carried out. The depth of the cavity recess can be comparable to wavelengths of interest, resulting in acoustic resonances that can be accounted for with calibration or reduced by acoustically treating the cavity.²³ Secondary acoustic sources also appear to be generated by airflow over the wall-mounted or strut-mounted in-flow array, and the CSM background subtraction method appears effective in reducing these sources since they are stationary.

1.3 Motivation and Objectives of this Study

Two primary objectives of the present study include:

- A. Design, assemble, calibrate, and test two configurations of a wall-mounted array system for cost effective and productive aeroacoustic measurements of moderate-scale test model aerodynamic investigations. The two configurations are array plate flush with the flow and array plate recessed behind porous windscreen.
- B. Apply the new array design to obtain acoustic measurements in a research test program for which high-fidelity aerodynamic measurements in a closed test-section were the primary research objective. In this study, the research test was a full scale Boeing 757 rudder with sweeping jet active flow control conducted by the NASA Environmentally Responsible Aviation (ERA) Program and Boeing for the NASA Aeronautics Research Mission Directorate (ARMD).

As will be noted in the following sections, these goals were successfully met by designing and implementing a new phased microphone array measurement system that included the following features:

- cost-effective, low-sensor count microphone array pattern (24 elements) optimized for accurate level measurements with significant background noise suppression over the frequency range of interest.
- modular wall mounting to allow placement of the array plate at most locations in the test section to sample the acoustic field as desired, either on the walls of a closed section wind-tunnel, or on the floor of a partially open facility.
- scalable system architecture to accommodate multiple fixed arrays (six were demonstrated, up to 20 possible with the existing data system) rather than a single traversing array to maximize test productivity and minimize facility occupancy cost. This approach will enable meaningful acoustic measurements on a non-interfering basis for research studies primarily conducted for high-fidelity aerodynamic measurements.

2. Array system design and test integration

2.1 Wind tunnel acoustic test operational environment for in-flow arrays

The challenge of developing and operating a microphone array system for wind tunnel aeroacoustic research depends on a wide range of factors including the facility configuration and specific test requirements for bandwidth, acoustic field coverage, source dynamic range, schedule, and available budget, to name a few. Many open jet acoustic research facilities have traversing acoustic sensors that are permanently installed since there is no flow interference and the traversing carriage can be moved out of the way for model installation and other measurements. Microphone arrays for closed test section wind tunnels used primarily for aerodynamic research are typically set-up temporarily for the duration of the test since the required sensor locations vary from test to test. Time needed to install, connect, check-out, calibrate, and remove equipment at the end of the test is nonproductive and needs to be minimized. These are some of the many factors affecting the design and layout of an acoustic array system for such a facility. A list of typical design, assembly, and operational factors that impact array system requirements includes the following:

A. Preparation set-up, and check-out:

- design, assemble, and calibrate array sensors pre-test
- determine optimal locations for placement of array(s), check for wind tunnel structural compatibility, aerodynamic interference, interference with service access to model, cable routing, access to sensors for check-out, calibration, replacement, accurate determination of array position and orientation relative to wind tunnel and test model.
- verification of channel assignments and signal quality
- in-situ calibrations with speaker sources in known locations, camera mounts and control systems for test images to superpose with beamform maps, verification of calibrations and corrections

B. Test operations

- communications with test team, triggering of acoustic data acquisition synchronous with acquisition of wind tunnel conditions and aerodynamic data, data processing and file management including routine processing of all acquired data as well as near-time processing of selected cases for test planning for the test in progress.
- periodic sensor recalibrations

C. Post-test

- post-test calibrations, check critical measurements
- removal of arrays, sensors, cables, instrumentation, data acquisition and processing equipment.
- full data processing, correction, and reporting

2.2 System configuration

Of the system requirements listed above, the major components of the acoustic array system that were achieved in this study include:

- 1) interfaces with the wind tunnel and aerodynamic data system. In this case, the acoustic data system needed to be completely independent of the wind tunnel aerodynamic data system during test operations. Critical wind tunnel parameters such as speed, temperature, etc were acquired as analog signals with the acoustic data for run-time analysis. The data was reprocessed with corrected wind-tunnel aerodynamic data following the completion of the test.
- 2) Application of the SADA-type small array in multiple fixed locations. The array panels were designed for rapid installation/connection and removal, and the individual sensors were accessible for service and mid-test calibrations.
- 3) Matlab/National Instruments (NI) based data acquisition software (developed by the co-author). The data acquisition system for this test consisted of 160 channels of NI PXI 4462 simultaneous 24-bit A/D operating at 102,400 samples/second rate, for six 24-element arrays (144 channels) and 16 channels for acquisition of wind tunnel and model conditions.
- 4) Spiral array pattern design for minimal sidelobe contamination over a wide frequency range.
- 5) Optimav BeamformInteractive[®] array processing software was used to generate near-time and archival source location maps, peak and integrated spectra. Most of the data was pre-processed using conventional beamform hemispheric mapping, as well as TIDY post processing for integrated levels. We are also comparing speed and accuracy of other available processing methods such as DAMAS and Functional Beamforming; results of these comparisons will be reported later.
- 6) VINCI²⁵ simulated imaging software to generate hemispheric test section images onto which the acoustic images were superposed.

2.3 Array pattern and wall fairing design

A wide variety of array microphone patterns such as simple crosses, concentric circles, and multi-armed spirals,^{1, 3, 12, 15} have been utilized for wind tunnel aeroacoustic research. Important performance metrics include spatial resolution, usable bandwidth, and ratio of peak to sidelobe response. Simulated annealing methods have also been used to optimize combinations of these factors.²² Post-processing with deconvolutional procedures such as DAMAS,⁸ TIDY,⁹ and other methods¹⁰ can also improve resolution and sidelobe suppression.

We selected a 3-armed equal-aperture spiral pattern with 8 sensors per arm (24 sensors per array), with minimum and maximum radii of 6 and 16.15 inches respectively for suitable performance in measuring source levels with background noise suppression over the design bandwidth of 150-20,000 Hz. MATLAB scripts published by Underbrink²⁴ were used to lay out the microphone locations and assess array conventional beamform response to simple source distributions. A sketch of the array microphone locations is presented in Fig. 4. Simulated response to two sources approximately 15° apart is presented in Fig. 5 for source frequencies of 2 and 16 kHz. At 2 kHz, the source separation is close to the Rayleigh limit. At 16 kHz, the sources are

fully resolved, and the clutter of sidelobes becomes more apparent. Location of acoustic sources was optimal between these frequencies, however the measured acoustic levels are accurate for frequencies well outside of this range.

The microphones selected for this array were Countryman B3 electret microphones with +/- 3 dB flat response from 20 to 20,000 Hz frequency range, and 150 dB maximum response. These microphones are also used in a turnkey 24-element array system (Array24jr) purchased previously from Optinav. The microphones were powered by 24-channel power supply/line drivers that were designed and built in-house and placed behind the installed array. More information on the microphone response, and a table of microphone locations are provided in Appendix 1. Details of the microphone power supplies and line drivers are provided in Appendix 2.

The arrays were designed to be mounted on the floor 20 ft under a model, or on the tunnel wall up to 40 ft from the centerline of the AEDC NFAC 40- by 80- ft wind tunnel, but can be adapted to other wind tunnels or test facilities. At the 20 and 40 ft distances, the array capture angles from a central point source are 7.6° and 3.8° respectively. These small capture angles lower the risk of measurement error due to source directionality or variable signal coherence over the array for distributed random sources.

Each array was mounted in an aluminum plate assembly that was hinged to a welded steel wall panel fairing that replaced a corresponding wall screen that covered one of the 42" deep liner cells of the wind tunnel, as shown in Fig. 6. The array plates were interchangeable to minimize fabrication costs, while the wall frames were designed for specific regions in the tunnel. The dimensions of the wall frames change slightly as the wind tunnel cross section area increases with downstream location to minimize streamwise pressure gradient as the boundary layer thickens.

Each array plate was 39.25" in the stream-wise direction, and 45.125" in the cross-stream direction. For the flush-mount configuration, the microphones were installed directly in this plate with microphone screens flush with the outer surface adjacent to tunnel flow. For the Kevlar wind-screen configuration, the microphones were mounted in a solid plate that was recessed 1/2" behind the screen. The wind-screen adjacent to the flow used 1.8 oz/sq. yard commercially available Kevlar sandwiched between two rings that had inner- and outer-diameters of 33.75 and 36.625 inches respectively. These screens were re-used from a large in-flow array built for a previous test.²¹ The wall fairing measured approximately 48 inches streamwise by 46 inches cross-stream and used the same four corner mounts as the wind tunnel liner screen that the array replaced during the test. The array panels were designed to withstand the full 300 kt speed ($M = 0.45$) of the tunnel to avoid the need to remove the panels during high speed aerodynamic testing.

2.4 Wind-off calibrations and corrections

Prior to the wind tunnel test, the arrays were tested and calibrated in the ARC 25- by 18 - by 11 foot high anechoic chamber that has freefield response from 250 Hz to 20 kHz. Each array was set up on a turntable in the anechoic chamber without the Kevlar wind-screen in front of a Tannoy CMS 501DC co-axial speaker source with an output bandwidth of 80 Hz to 50kHz. (0 to -3 dB response) as shown in Fig. 7 for the 90°

(broadside) condition. The response measurements were acquired every 15°, and were referenced to a G.R.A.S. 40BF ¼” free-field condenser microphone located in the array center position with the array removed, before and after array calibration. In Fig. 7, the blue side extensions simulate the solid leading-and trailing edges of the array panel as mounted in the wind tunnel. The array correction based on conventional beamform hemispheric peak is shown in the graph to the right of Fig. 7. From 160 Hz to 20 kHz the correction falls within a band of -5 to -8 dB. Above 20 kHz, the correction increases rapidly due to the 20 kHz bandwidth of the electret array microphones relative to the G.R.A.S condenser microphone that has a response bandwidth of 4 Hz to 100 kHz (+/- 2dB). Two curves are shown, with (blue) and without (red) applying a phase calibration of the array microphones from a reference speaker source. This phase calibration was not applied to the wind tunnel measurements since it was less than 1 dB across the frequency range. For the wind tunnel test, the array plate response calibration seen in Fig. 7 was also not applied to measurements of background noise; instead a uniform - 6.01 dB correction was used to account for the effect of the plate mounting. Further quantification of this effect is planned for future study to improve the accuracy of array level measurements for aeroacoustic sources.

The effect of the Kevlar wind screen on directional frequency response of one of the arrays is shown in Fig. 8 for 90°(broadside) orientation. This correction was also measured every 15°. This effect resulted in a correction for 90° source emission between – 2 dB at 160 Hz to a peak of +3.8 dB at 12 kHz. Time constraints precluded obtaining similar measurements for all of the arrays prior to the wind tunnel test. Instead, the Kevlar windscreen effect on array frequency response was measured after installation in the wind-tunnel with an omnidirectional speaker source on the tunnel centerline. Wind-off measurements of the speaker source with windscreens installed were followed directly by measurements with the windscreens removed to quantify the effect of the Kevlar in-situ. Further research is planned to determine the effect of windscreen tension, humidity, etc. on this effect, as well as the effectiveness of other wind screen materials and microphone mounting configurations.

3. Wind tunnel study of array background noise

3.1 Installation and set-up

The flush array plate and Kevlar wind screen arrays are shown mounted in the east test section wall of the AEDC NFAC 40- by 80-Ft Wind Tunnel in Fig. 9a. Each array was installed by removing a porous face sheet frame from one of the 42 inch deep liner cells and securing the array frame to four corner bolts. The anechoic wedges in the array cell were not disturbed since the array hardware projected only an inch lower than the original porous cell cover. A 24-channel microphone power supply/line driver unit was located behind each array (see Appendix 2). This unit was powered by +/- 15V DC supply located under the wind tunnel turntable with the data acquisition hardware. The power supply cable was bundled with 25 RG174 coaxial cables approximately 140 ft. long for each array. The cables were secured to ¾” electrical conduit that was attached to the tunnel wall.

Also shown in Fig. 9 is a high frequency disk array with 24 condenser microphones mounted on an 18 inch strut below and to the right of the flush plate array. The design and fabrication of this array was supported by the NASA ARMD Aeronautical Sciences

Project. The array pattern in this sensor is a $\frac{1}{4}$ scale version of the wall-mounted array. This array was designed for higher frequency response with $\frac{1}{4}$ " G.R.A.S. condenser microphones and with the fairing placed above the wall boundary layer to minimize turbulent scattering of the acoustic waves from the target source. Analysis of data from this array is in progress and will be reported separately.

The wall-mounted arrays were tested for empty-tunnel background noise to the maximum wind tunnel speed of 300 kt ($M = 0.45$). Following these measurements, a calibration speaker fairing and the strut mounted disk array were installed for wind-on speaker measurements to 200 kt ($M = 0.3$). In both test configurations, measurements were acquired with the tunnel drive system in variable frequency mode (quieter operation up to 130 kts) as well as fixed 60 Hz utility mode for higher speeds. Measurements were acquired for tunnel Mach number increments of 0.05 for each range for increasing and decreasing speed, and for duplicate test runs separated by full tunnel stop and restart.

3.2 Wind-on speaker source measurements

At each Mach number (0.05 to 0.3), the speaker power was varied from 0, 32, 3.6, 0.32, 0.036 watts with a SRS DS360 pink noise source input and Mackie 100 W power amplifier connected to the center speaker. Following the pink noise source measurements, response to a 32W 500 Hz square wave was measured to assess the extent to which boundary-layer turbulence degraded the narrow-band response of the array. Analysis of the square wave response is currently in progress.

Typical response of the B2 Kevlar windscreen array at 100 kts ($M = 0.15$) to various power settings of the pink noise source is shown in Fig. 10, left, and compared with the background noise level of the strut mounted G.R.A.S. 40BF free-field microphone with quiet Flow Induced Tone Eliminating (FITE) nosecone measured by C. Allen²⁶ in a previous study (black line). The array noise was measured during utility fan drive mode (60 Hz power), and a tunnel drive tone is apparent at 240 Hz in the array data. The FITE microphone data was obtained at the same tunnel speed with the quieter variable drive frequency mode. The background noise level is higher for the FITE microphone than for the array except at the drive frequency tone. The 32W speaker signal (red line) is above the background level from 2 to 15 kHz, the 3.6 W signal (green) is visible only from 6 to 11 kHz. The signal from lower speaker power settings down to 0 W is below the background noise of the array at this speed. The array background noise is lower than the quiet FITE microphone level by levels that vary from 5 dB at 400Hz to 15 dB at 10 kHz.

In Fig. 10, right, the same data was reprocessed after first subtracting the time-averaged cross-spectral-matrix (CSM) of the data for 0 W speaker from each of the other non-zero power measurements. This process further reduces the background noise level by eliminating stationary noise sources due to the tunnel drive at 240 Hz, noise from the speaker strut and fairing, and local noise from the interaction of the wall turbulent boundary layer with the wall-mounted fairing and wind screen. In this case the 32 W signal can be observed from 400 Hz to 16 kHz, and the subtracted background level is lower than the quiet FITE microphone data by levels that vary from 8 dB at 400 Hz to 20 dB at 10 kHz. Direct background subtraction is one of the noise cancelling methods suggested by Blacodon, et al.¹⁷ The direct background subtraction is most effective for

target sources that can be varied during the same wind-tunnel run, as in the case of compressed air actuators or slot blowing, as will be discussed later in this report.

Fig. 11 compares the 100 kt background noise levels measured with and without background noise CSM subtraction for a Kevlar windscreen array T2 and flush plate array K2. The T2 array was upstream of the flush plate array K2 at the same height above tunnel floor, and had background levels similar to the B2 array discussed previously. The T2 wind screen array exhibits lower background with CSM background subtraction (solid green line) than without (dashed green line). In comparison, the flush plate array K2 exhibits some cancellation of the tunnel drive noise with CSM background subtraction (solid red line) but otherwise is about 3 dB louder than the case with no CSM background subtraction (dashed red line) above 1 kHz. This suggests that the flush plate background signal is dominated by turbulent boundary layer pressure fluctuations above 1 kHz, and that background CSM subtraction method that reduces radiated broadband background noise from in-flow struts and flow interactions local to the array is not effective for the flush-mount array.

For comparison, background noise measurements with CSM background subtraction of the strut mounted fairing array with 48 sensors (see Fig. 2d, far left) is shown at the same speed as the blue solid line in Fig. 11. The background for A48 is lower than for the wall-mounted T2 from 0 to 6 dB. This may be related to the thinner boundary layer for the in-flow fairing array vs the wall-mounted array (1 inch vs 18 inches boundary layer thickness). Note also a high-frequency feature that peaks at 25 kHz for the fairing array A48 versus 15 kHz for the wall array T2. This feature may be related to local speed-dependent noise from boundary-layer turbulence “scrubbing” the surface of the Kevlar wind screen used in both arrays. The high-frequency feature was suppressed by Fleury et al. by using stainless steel screen rather than Kevlar²².

3.3 Empty-tunnel background noise measurements to 300 kts, (M=0.45)

Comparisons of background noise spectra with CSM background subtraction are presented in Fig. 12 for tunnel speeds of 100 kts ($M = 0.15$), 166 kts ($M = 0.25$), 233 kts ($M = 0.35$) and 300 kts ($M = 0.45$). For each graph, spectra are shown for the quiet FITE microphone (black curve), wall array B2 (red curve, open symbols), array B2 with CSM background subtractions (red curve, closed symbols), and in-flow array A48 with CSM background subtraction (blue curve for $M = 0.15, 0.25$). In each case the array background spectra without CSM background subtraction are quieter than for the quiet FITE microphone over most of the frequency range, and CSM background subtraction further reduces the noise level. B2 array levels are generally louder than the A48 levels at low frequencies for $M = 0.15$, but the difference is less pronounced at $M = 0.25$.

4. Research application: NASA/Boeing active rudder acoustic measurements

Within the time frame of research for this seedling study, the ARMD Environmentally Responsible Aviation (ERA) project with industry and academic partners began preparations for a wind tunnel test of a flight component Boeing 757 rudder equipped with sweeping jet active flow control to improve lift control at high rudder deflections by maintaining attached flow with enhanced mixing. The test article was modified with the installation of 37 actuators just forward of the rudder hinge line, and the flow rate through

each actuator was independently adjusted with analog valve control of individual actuator plenum pressures. This test demonstrated that by increasing the maximum available lift coefficient, rudder size and weight could be reduced while maintaining adequate yaw control in the event of loss of one engine for a twin-engine transport during take-off.²⁷

Acoustic measurements of this configuration had not been acquired in previous studies, and were not planned for this test due to added cost and the low priority of noise control for a flight emergency control system. Since the two arrays developed by the present study would be available for this test, ARMD Fixed Wing Project approved a proposal to build four additional arrays and support acquisition of the acoustic data for the study. The wind-tunnel test team also approved acoustic data acquisition on a non-interference basis with regard to either affecting the aerodynamic environment or slowing the test schedule. The acoustic measurements will be used to estimate sideline noise levels for a planned flight demonstration, and to estimate ground noise levels and shielding for potential applications of the sweeping jet actuator to augment wing high-lift effectiveness.²⁸

In addition to the B2 (Kevlar windscreen) and K2 (flush plate) arrays described previously, four additional arrays with Kevlar windscreen were built and installed at the same elevation as shown in Fig. 13. Array T2 was added upstream from K2 on the actuator side (right) of the model, B25, K25, and T25 were added non the non-actuated side (left). Imaging for this figure and the beamform map images discussed below were generated by the VINCI test image generation tool developed at NASA ARC.²⁵

Data from this test are being analyzed for a later report, however some preliminary results demonstrate the successful design and application of the new array systems. Fig. 14 presents hemispheric conventional beamform maps from the B2 array for selected 1/3-octave bands at 250, 500, 1000, 2000, 4000, and 8000 Hz. For these measurements, the test configuration was with six of 37 actuators active, 0° model yaw and rudder deflection at 100 kts. Relatively high noise regions (bright areas) associated with the six actuators and a reflection off the lower fairing are seen at the highest frequency. At lower frequencies the noise areas increase in size but remain centered on the actuator line mid-point. The oval shapes to the left and right of each map indicate the upstream and downstream limits of the test section. The beamform maps were processed after CSM background noise subtraction, using for the background condition the same test configuration except for all actuators being turned off. For conventional beamforming without CSM background noise subtraction, the actuator noise areas were still visible, but frequency-dependent noise from the tunnel drive system was also visible.

Fig. 15 compares 1/3-octave spectra of relative peak and integrated beamform levels from the array measurements of the model with the same configuration described previously. The origin of each graph is set to the same level for comparison between arrays. Common spectral features include peaks at 250 Hz and 500 Hz associated with the sweeping jet fundamental and first-harmonic frequencies, followed by rising broadband noise associated with the actuator jets peaking at about 15 kHz. The upper black curve in each graph is the spectrum of the center-most microphone from each array. The green curve is the hemispheric peak of the conventional beamform map with CSM background subtraction, while the red curve with open symbols is the hemispheric peak of the map using TIDY deconvolutional post-processing. The solid red curve is the

hemispheric integration of levels over the TIDY beamform map; it is close to the peak level at 1 kHz and lower frequencies for which the shape of the noise region is nearly circular, but increases by 8-10 dB relative to the peak level as the array is able to resolve the linear shape of the line of source actuators. For these frequencies and for the 6 active actuators, the integrated level should be $10 \cdot \log(6)$ or 7.8 dB greater than the level of one of the actuators. The blue curve is the estimated background noise limit for measurements using CSM background noise subtraction.

Note that the flush plate array K2 has sufficient dynamic range to measure the actuator noise, but that the spectra for the center microphone and estimated background noise limit are 15 dB or more higher than for the arrays B2 and T2 with Kevlar wind-screen. This comparison is consistent with the empty tunnel background measurements presented earlier in Fig. 13. We note previous tests showed that the flush array design to have higher background noise levels than for the windscreen configuration, but was included in this study to provide a baseline measure of the un-attenuated background noise level as a reference. Also apparent in Fig. 15 are directional differences in the relative levels of the 250 Hz fundamental and the 500 Hz harmonic between the three arrays.

Fig. 16 presents hemispheric conventional beamform maps from array B25 at the downstream location on the non-actuated side of the model. Model associated noise is apparent at all frequencies. At 2 kHz and higher, a noise source at the base of the rudder is probably associated with the actuator air supply, as well as a possible reflection from the actuator-side tunnel wall that appears in the same location for the highest three frequencies. Fig. 17 presents peak and integrated spectra measured by arrays B25, K25, and T25 on the non-actuated side of the tunnel with the same level reference at the origin of the graph as in Fig. 15, and with CSM background noise subtraction. Although the levels are significantly lower than for the actuator-side measurements, the 250 Hz and 500 Hz peaks are discernable. The broadband jet noise is attenuated significantly but is still above the background. Note that the hemispheric conventional beamform peak (green line) is unable to measure actuator noise below 2 kHz, but that the deconvolutional post-processing with TIDY is able to discern the noise spectra to the lowest frequency band centered at 160 Hz.

These measurements validate the use of the wall-mounted arrays to characterize the acoustic field of the active rudder model in the presence of high background noise from the adjacent wall boundary layer and the tunnel drive sources. The use of passive and active noise mitigation methods (wind screens and CSM background subtraction respectively) were effective and necessary to capture the source spectra.

5. Concluding Remarks

A new wall mounted array configuration was designed, assembled, calibrated and tested in the acoustically treated AEDC NFAC 40- by 80-Ft Wind Tunnel to characterize reductions in background noise achieved with porous wind screens and advanced array processing methods. The principal background noise sources are the tunnel drive system at low frequencies, broadband noise from in-flow struts, and hydrodynamic pressure fluctuations from the wall- or floor-boundary layer. These sources are typical of corresponding sources in other closed test-section or partially open facilities. Two

configurations were tested to a speed of 300 kts ($M = 0.45$): 24 electret microphones in a spiral pattern within a 32 inch diameter circle on a solid plate flush with the flow, and the same pattern on a plate recessed $\frac{1}{2}$ " behind a Kevlar windscreen that was flush with the flow. The windscreen array demonstrated background noise reductions of 15-25 dB relative to an in-flow microphone with a quiet nosecone, while the flush-plate array demonstrated reductions that were less pronounced. The microphones demonstrated useful measurement of peak and spatially integrated levels of low intensity sources typical of new quiet vehicle configurations over a bandwidth of 160 to 20,000 Hz.

Four additional arrays with windscreens were built, calibrated, and installed in the wind tunnel for measurement of a flight-hardware Boeing 757 rudder with sweeping jet active flow control to increase the maximum control effectiveness needed during an engine-out emergency. These measurements were the first acoustic characterization of this configuration at any scale, and will be used to help plan a flight-demonstration of the concept in the near future. Although the arrays were designed for accurate level measurement rather than high-resolution source location, the arrays were able to discriminate individual control actuators at high frequencies.

Additional efforts to further reduce the background noise are being planned and will proceed with model scale experiments in the anechoic chamber at ARC. Modification of a nozzle capable of simulating flow with variable boundary layer thickness is in progress. This nozzle will be used to optimize the wind screen and microphone support configurations for accurate level measurement and minimum background noise.

References

1. Dougherty, R. P., "Beamforming in Acoustic Testing," in *Aeroacoustic Measurements*, T.J. Mueller, ed., Springer, 2002.
2. Mosher, M., "Phased Arrays for Aeroacoustic Testing: Theoretical Development," AIAA-96-1713, 2nd AIAA/CEAS Aeroacoustics Conf., State College, PA, May 6-8, 1986.
3. Humphreys, W.M., and Brooks, T.F., "Noise Spectra and Directivity for a Scale-Model Landing Gear," AIAA-2007-3458, 13th AIAA/CEAS Aeroacoustics Conf., Rome, Italy, May 21-23, 2007.
4. Heath, S.L., et al, "Hybrid Wing Body Aircraft Acoustic Test Preparations and Facility Upgrades," AIAA2013-2623, 28th AIAA Aerodynamic Measurement Technology, Ground Testing, and Flight Testing Conf., June 24-27, 2013, San Diego, CA.
5. Stoker, R.W., Underbrink, J.R., and Neubert, G.R., "Investigations of Airframe Noise in Pressurized Wind Tunnels," AIAA-2001-2107, 7th AIAA/CEAS Aeroacoustics Conf., Maastricht, The Netherlands, 2001, May 28-30, 2001
6. Burnside, N.J., and Horne, W.C., "Acoustic Surveys of a Scaled-Model CESTOL Transport Aircraft in Static and Forward Speed Conditions," AIAA-2012-2231, 18th AIAA/CEAS Aeroacoustics Conf., June 4-6, Colorado Springs, CO.
7. Horne, W.C., and Burnside, N.J., "AMELIA CESTOL Test: Acoustic Characteristics of Circulation Control Wing and Leading- and Trailing-Edge Slot Blowing," AIAA2013-0978, 51st AIAA Aerospace Sciences Meeting and Exhibit, Grapevine, TX, Jan. 7-10, 2013.
8. Brooks, T.F., and Humphreys, W.M., "A Deconvolutional Approach for the Mapping of Acoustic Sources (DAMAS) determined from phased microphone arrays," AIAA-2004-2954, 10th AIAA/CEAS Aeroacoustics Conf., May 10-12, 2004, Manchester, UK.
9. Dougherty, R.P., and Podboy, G.C., "Improved Phased Array Imaging of a Model Jet," AIAA-2009-3186, 15th AIAA/CEAS Aeroacoustics Conf., May 11-13, 2009, Miami, FL.
10. Dougherty, R.P., "Functional Beamforming," BeBeC-2014-01, Berlin Beamforming Conf., Feb. 19-20, 2014, Berlin, Ger.
11. Guo, Y., Brusniak, L., Czech, M., and Thomas, R.H., "Hybrid Wind-Body Aircraft Slat Noise," AIAA J., vol. 51, no. 12, Dec. 2013, pp 2935-2945.
12. Panda, J., Mosher, R.N., and Porter, B.J., "Identification of Noise Sources During Rocket Engine Test Firings and a Rocket Launch Using a Microphone Phased-Array," NASA/TM-2013-216625, Dec. 2013.

13. Dougherty, R.P., "Turbulent Decorrelation of Aeroacoustic Phased Arrays: Lessons from Atmospheric Science and Astronomy," AIAA-2003-3200, 90th AIAA/CEAS Aeroacoustics Conf. and Exhibit, May 12-14, Hilton Head, SC.
14. Pires, L.S., Dougherty, R.P., Gerges, S.N.Y., and Catalano, F., "Predicting Turbulent Decorrelation in Acoustic Phased Array," AIAA-2012-0387, 50th AIAA Aerospace Sciences Meeting, Jan. 9-12, 2012, Nashville, TN.
15. Brooks, T.F., and Humphreys, Jr., W.M., "Effect of Directional Array Size on the Measurement of Airframe Noise Components," AIAA-99-1958, 5th AIAA/CEAS Aeroacoustics Conference, May 10-12, 1999, Bellevue, WA.
16. Underbrink, J.R., "Aeroacoustic Phased Array Testing in Low Speed Wind Tunnels," in Aeroacoustic Measurements, T.J. Mueller, ed., Springer, 2002.
17. Humphreys, W. et al "Design and Use of Microphone Directional Arrays for Aeroacoustic Measurements," AIAA-1998-471, 36th AIAA Aerospace Sciences Meeting and Exhibit, Jan. 12-15, 1998, Reno, NV.
18. Blacodon, D., "Array Processing for Noisy Data: Application for Open and Closed Wind Tunnels", AIAA J., vol. 49, no. 1, Jan. 2011.
19. Spalt, T.B., Fuller, C.R., Brooks, T.F., and Huphreys, Jr., W.M., "A Background Noise Reduction Technique using Adaptive Noise Cancellation for Microphone Arrays," AIAA-2011-2715, 17th AIAA/CEAS Aeroacoustics Conf., June 5-8, Portland, OR.
20. Koop, L, and Ehrenfried, K. , "Microphone-Array Processing for Wind-Tunnel Measurements with Strong Background Noise," AIAA-2008-2907, 14th AIAA/CEAS Aeroacoustics Conf., 2008, Vancouver, Can.
21. Jaeger, S.M., Horne, W.C., and Allen, C.S., "Effect of Surface Treatment on Array Microphone Self-Noise," AIAA-2000-1937, 6th AIAA/CEAS Aeroacoustics Conf. and Exhibit, June 12-14, 2000, Lahaina, NV.
22. Burnside, N.J., Jaeger, S.M., Reiner, B.F., Horne, W.C., and Soderman, P.T., "Array Design and Performance for a Large Scale Airframe Noise Study", AIAA-2002-2576, 8th AIAA/CEAS Aeroacoustics Conf. and Exhibit, 2002.
23. Fleury, V., Coste, L., Davy, R., Mignosi, A., Cariou, C., and Prosper, J.M., "Optimization of Microphone Array Wall Mountings in Closed-Section Wind Tunnels", AIAA J., vol. 50, no.11, Nov., 2012.
24. Underbrink, J.R., "Practical Considerations in Focused Array Design For Passive Broad-band Source Mapping Applications," Master of Engineering Paper, The Pennsylvania State University, 1995.
25. Kushner, L.K. and Schairer, E.T., "Planning Image-Based Measurements in Wind Tunnels by Virtual Imaging," AIAA Paper 2011-0930, presented at 49th AIAA Aerospace Sciences Meeting and Exhibit, Orlando, FL, Jan., 2011.

26. Allen, C.S., Jaeger, S.M., Soderman, P.T., "Background Noise Sources and Levels in the NASA Ames 40- by 80-Foot Wind Tunnel at the Turn of the Century: A Status Report," NASA/TP-2003-212259, Nov. 2003.

27. Seele, R., Graff, E., Lin, J., and Wygnanski, I., "Performance Enhancement of a Vertical Tail Model with Sweeping Jet Actuators," AIAA-2013-0411, 51st AIAA Aerospace Sciences Meeting, Jan. 07-10, 2013, Grapevine, TX.

28. Tewes, P., Taubert, L, and Wygnanski, II, "On the Use of Sweeping Jets to Augment the Lift of a λ -Wing", AIAA-2010-4689, 28th AIAA Applied Aerodynamics Conf., June 28 – July1, 2010, Chicago, II.

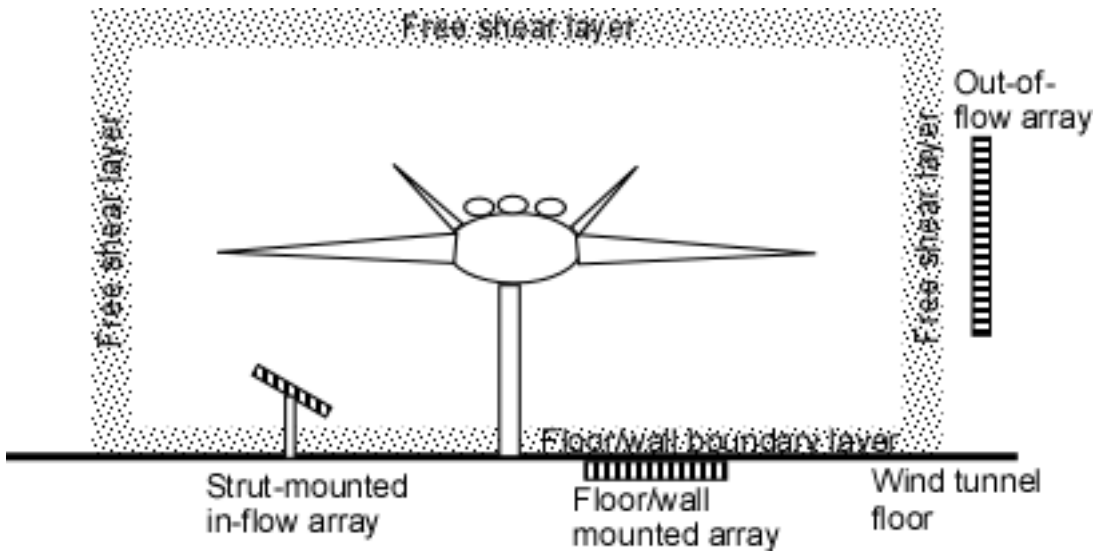
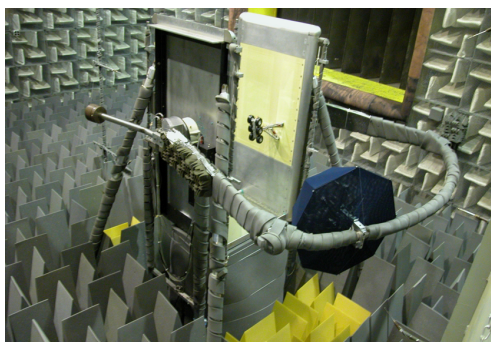
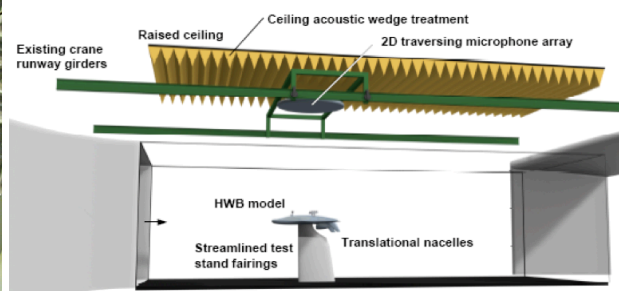


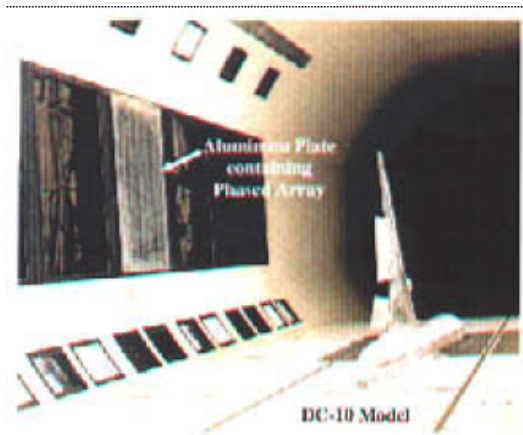
Fig. 1. Aeroacoustic test set-up with phased microphone arrays.



a) QFF MADA out-of-flow array



b) 14'x22' wind tunnel out-of-flow array



c) 12' PWT wall-mounted array



d) 40'x80' strut-mounted in-flow array

Fig. 2. Recent array configurations for aeroacoustic research, open and closed section wind tunnels.

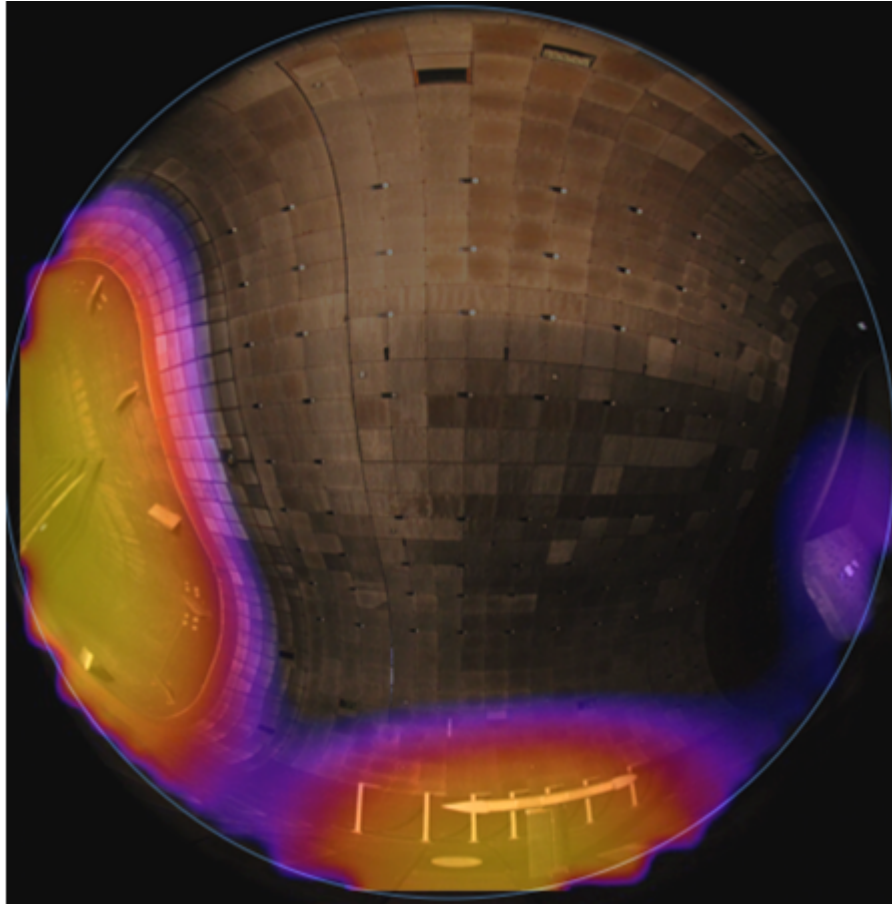


Fig. 3. 180° Fisheye image and superposed conventional beamform map of NFAC AEDC 40x80 wind tunnel at 100 kts, 800 Hz 1/3 octave band, with tunnel drive noise seen from downstream and upstream. Broadside noise is also seen from the 7 microphone struts in front of the array. The white structure in front of the microphone struts is the speaker fairing on a separate strut.

Array file: a24c5_0a.txt, 24 elem., Max. rad. = 16.1553 in.

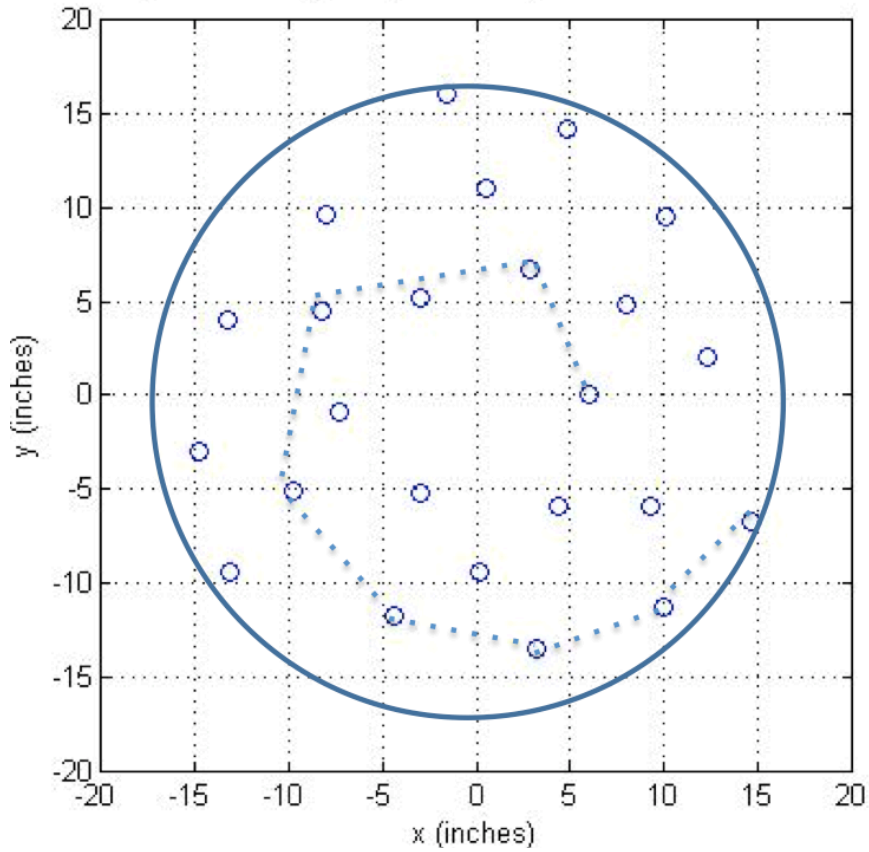


Fig. 4. Spiral array layout, 24 microphones, 32" diameter pattern.

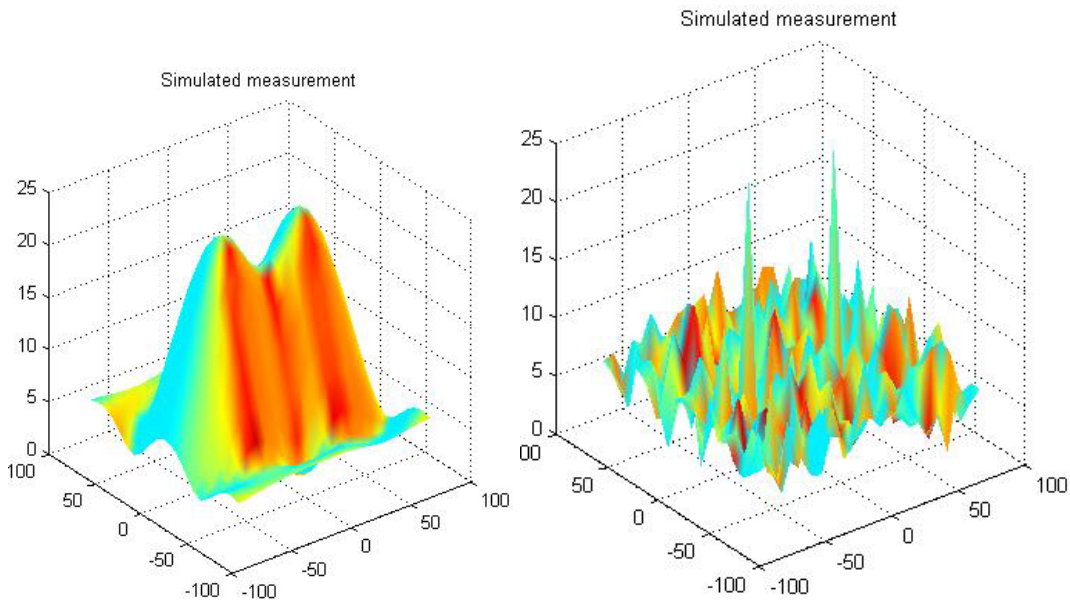


Fig. 5. Array response (conventional beam forming) to two sources with 15° separation at 2 kHz (left) and 16 kHz (right).

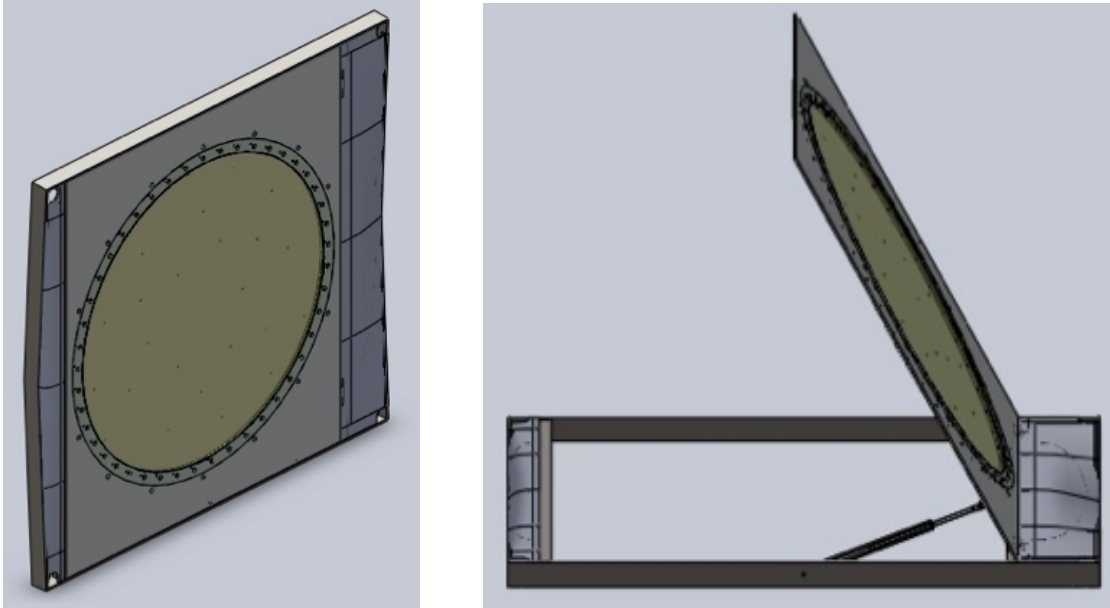


Fig. 6 Wall fairing design, Kevlar wind-screen configuration.

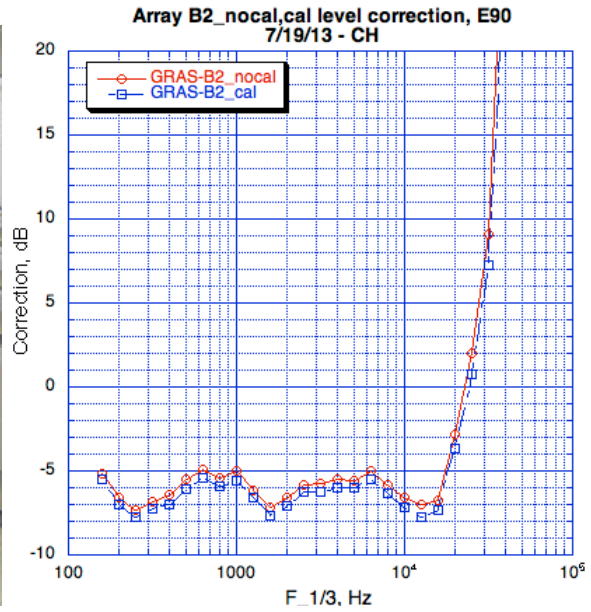


Fig. 7. Anechoic chamber directional calibration set-up and measured correction (Kevlar removed).

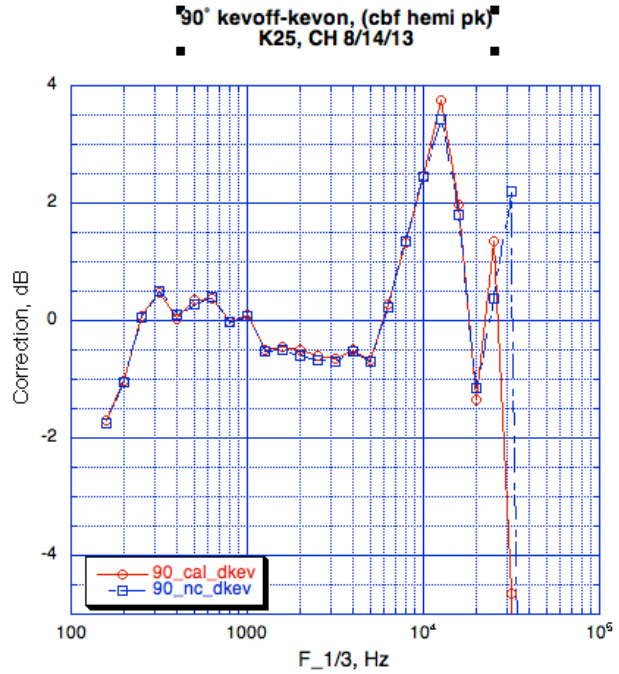
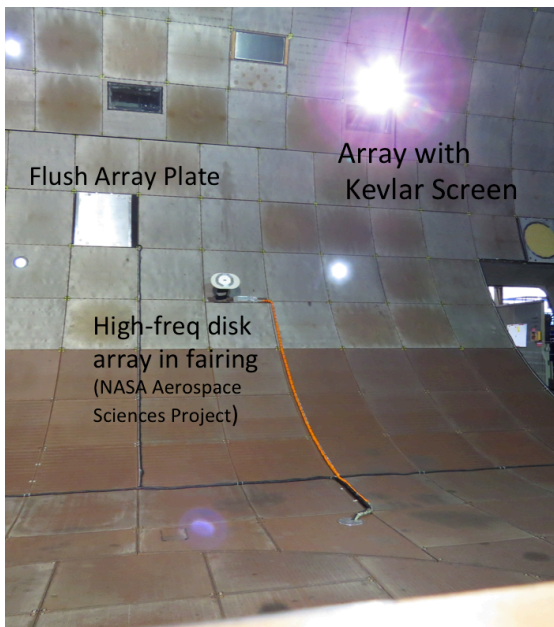


Fig. 8 Anechoic chamber Kevlar effect calibration set-up (left) and measured correction for K25 (right).



a) view of flush array K2 and Kevlar windscreen array B2. Also shown is strut-mounted disk array D3

b) speaker fairing source. Speakers are coaxial 2-element speakers with 80 Hz - 54 kHz response

Fig. 9. B2 (Kevlar windscreen) and K2 array and speaker source set-up in wind tunnel.

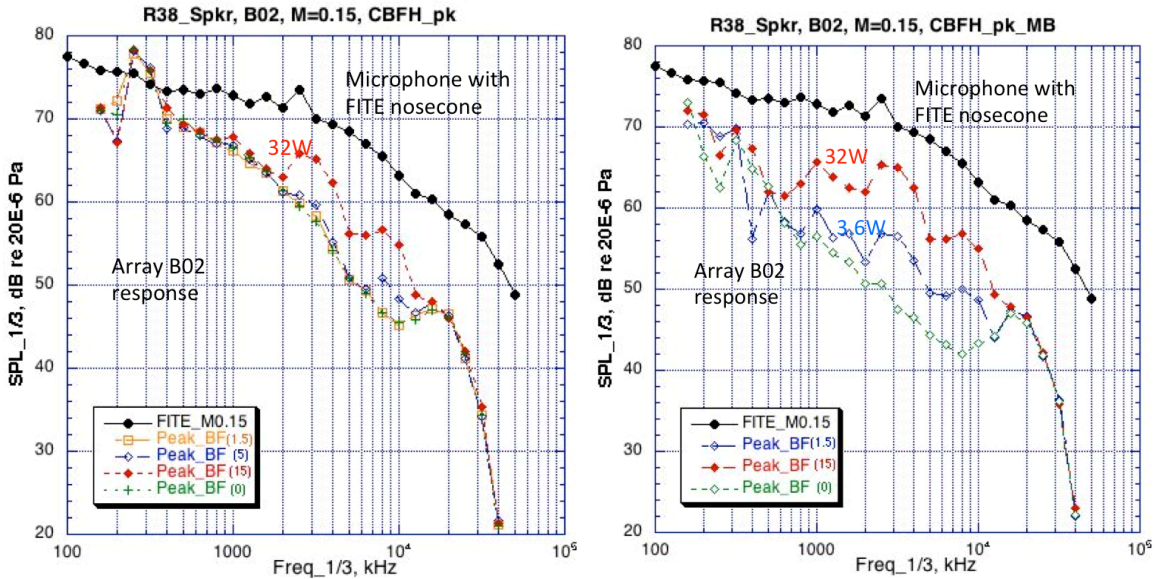


Fig. 10. Speaker response - array B02 peak response to speaker source with conventional beamforming (left) and with conventional beamforming after subtracting the cross spectral matrix of a condition with speaker off. Tunnel speed = 100 kts

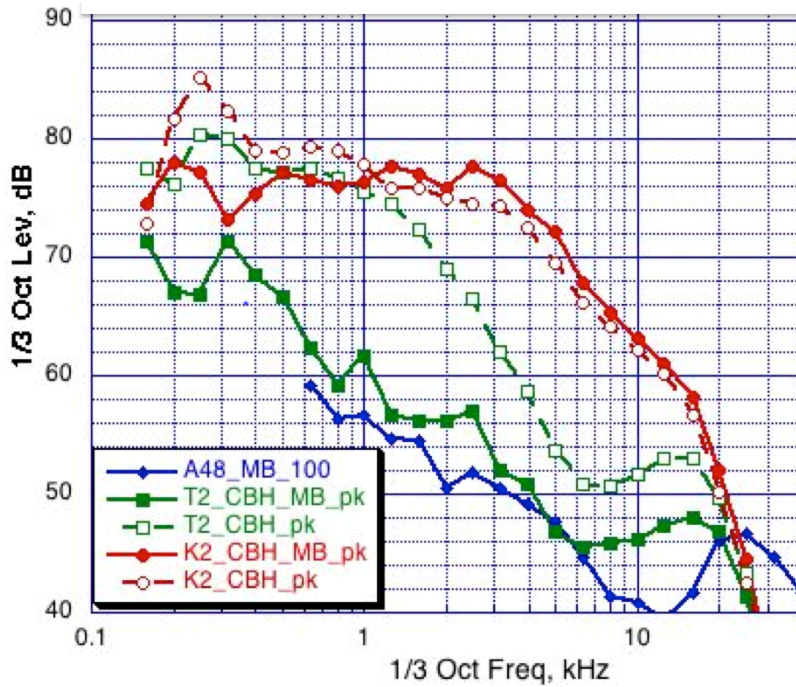


Fig. 11. Comparison of 100 kt peak background noise levels for array T2(green- Kevlar screen) and K2 (red- flush plate) with and without background noise subtraction. Also shown is background noise for in-flow array A48 (blue – Kevlar screen) with background noise subtraction.

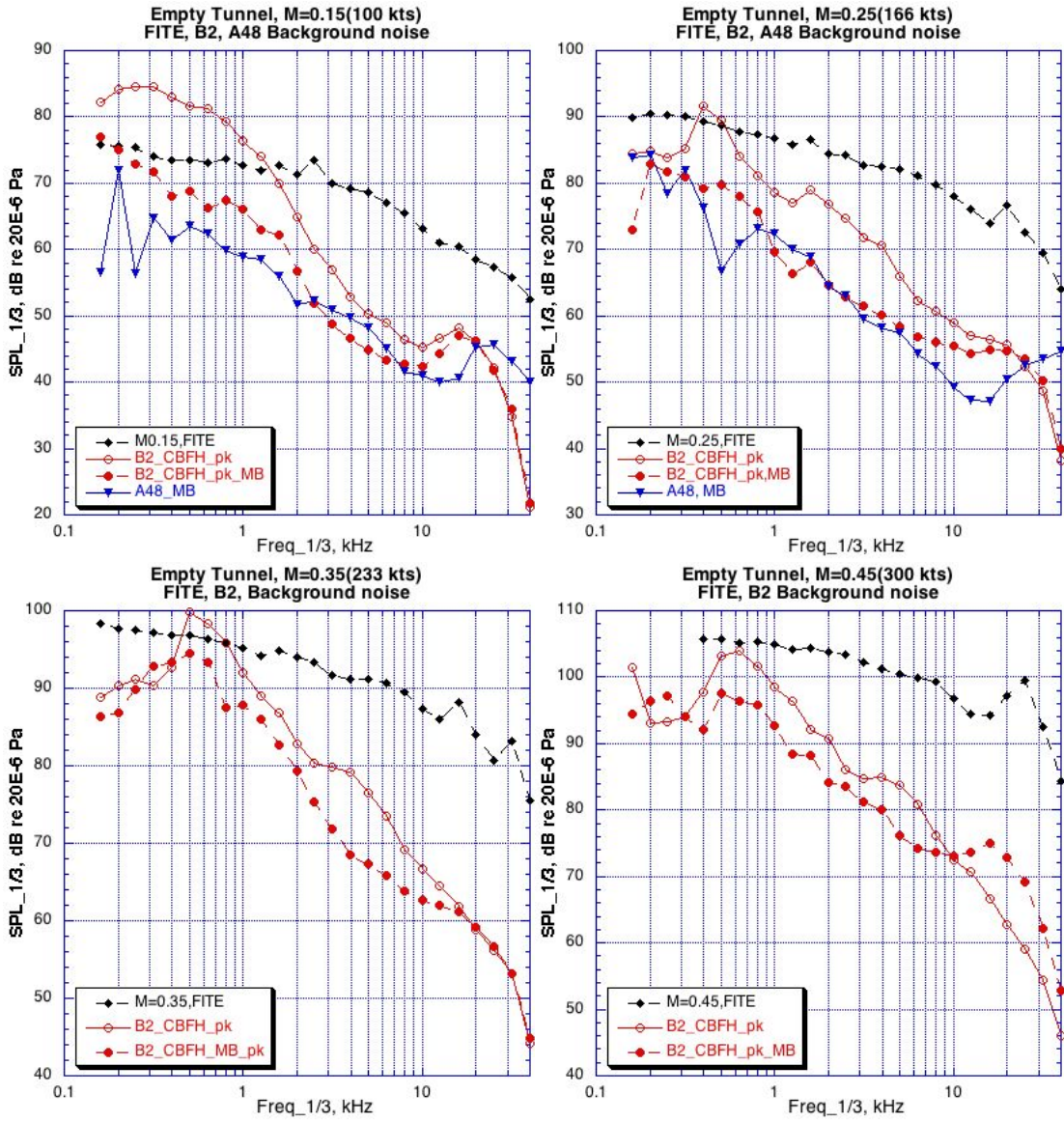


Fig. 12. Array background noise at M = 0.15, 0.25, 0.35, 0.45

-black: FITE microphone (Allen, 2003)

- red open: B2 conventional beamform hemispheric peak

-red closed: B2 conventional beamform hemispheric peak, background subtract

-blue: A48 conventional beamform hemispheric peak, background subtract

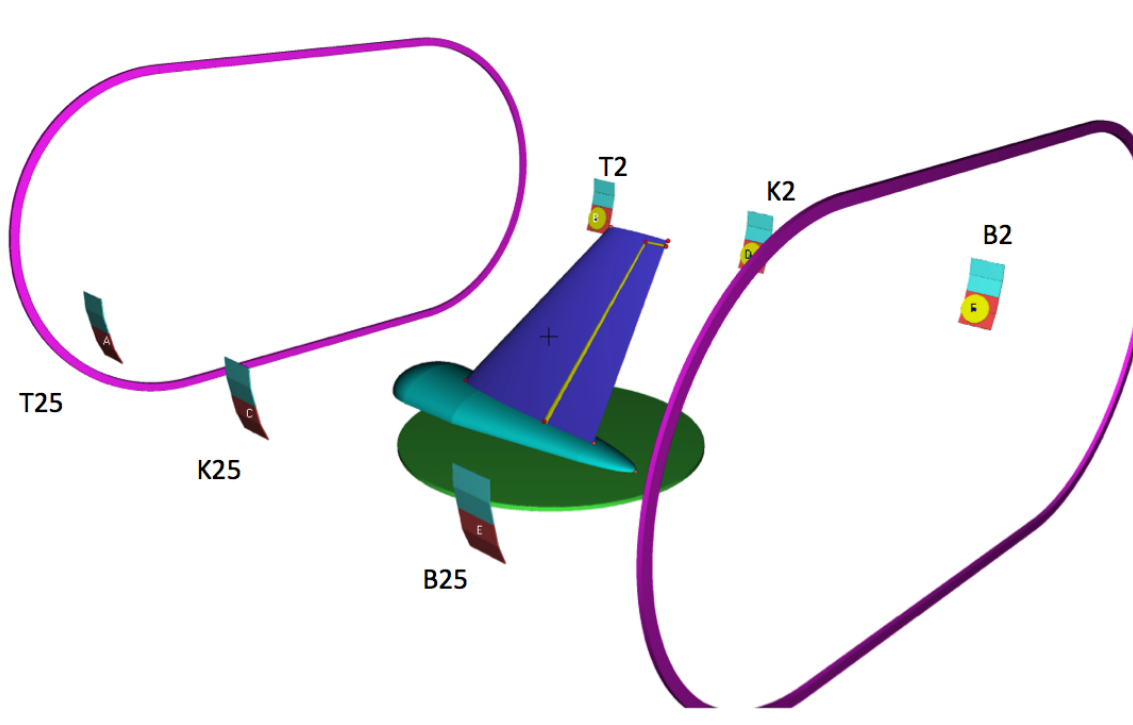


Fig. 13 VINCI image of wall-mounted arrays for acoustic measurements of NASA/Boeing full-scale 757 active flow control rudder. Arrays T2, K2, and B2 are on the same side as the sweeping jet actuators.

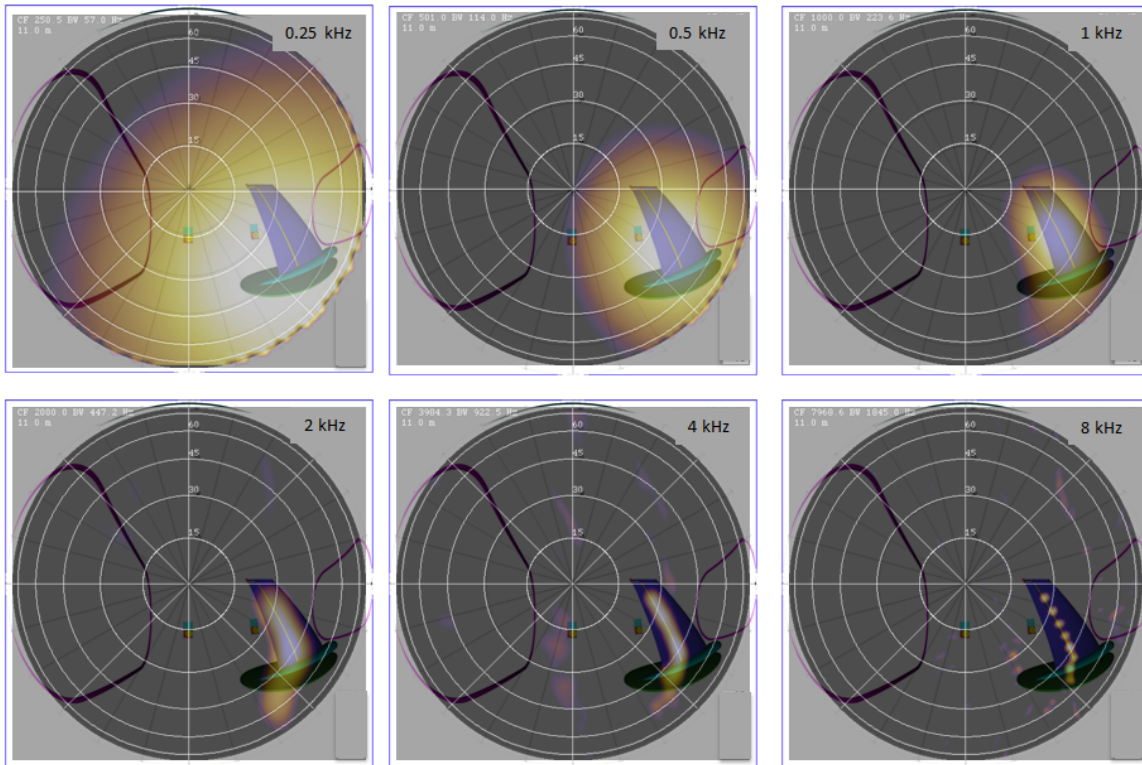


Fig. 14. 757 active rudder actuator-side beamforms maps from array B2 at 100 kts, 6 actuators active, conventional beamform process with CSM background noise subtraction.

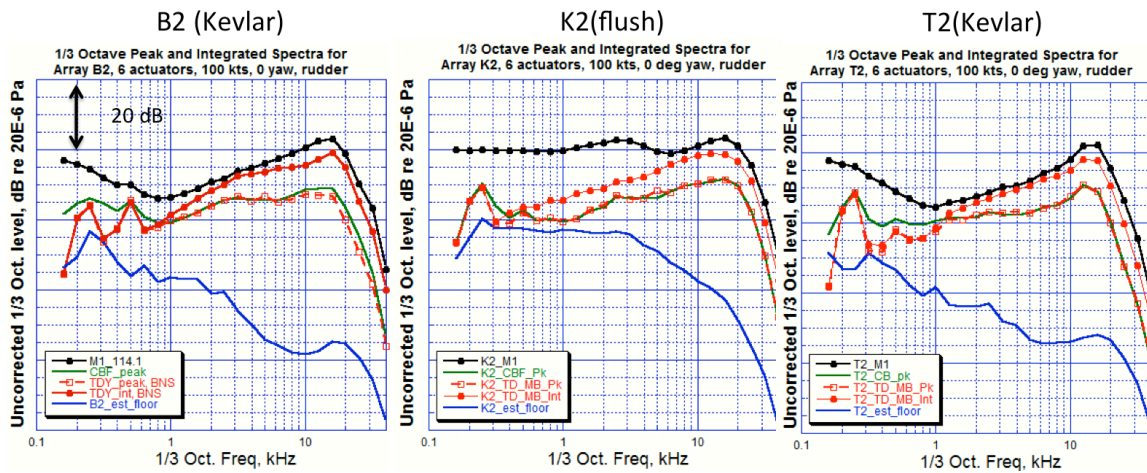


Fig 15. 757 active rudder actuator-side sample spectra, 100 kts, 6 actuators active.

- black: microphone 1
- blue: estimated peak array background noise level (background subtract)
- green – conventional beamform peak (background subtract)
- red open – TIDY process peak (background subtract)
- red closed – TIDY process hemispheric integral (background subtract)

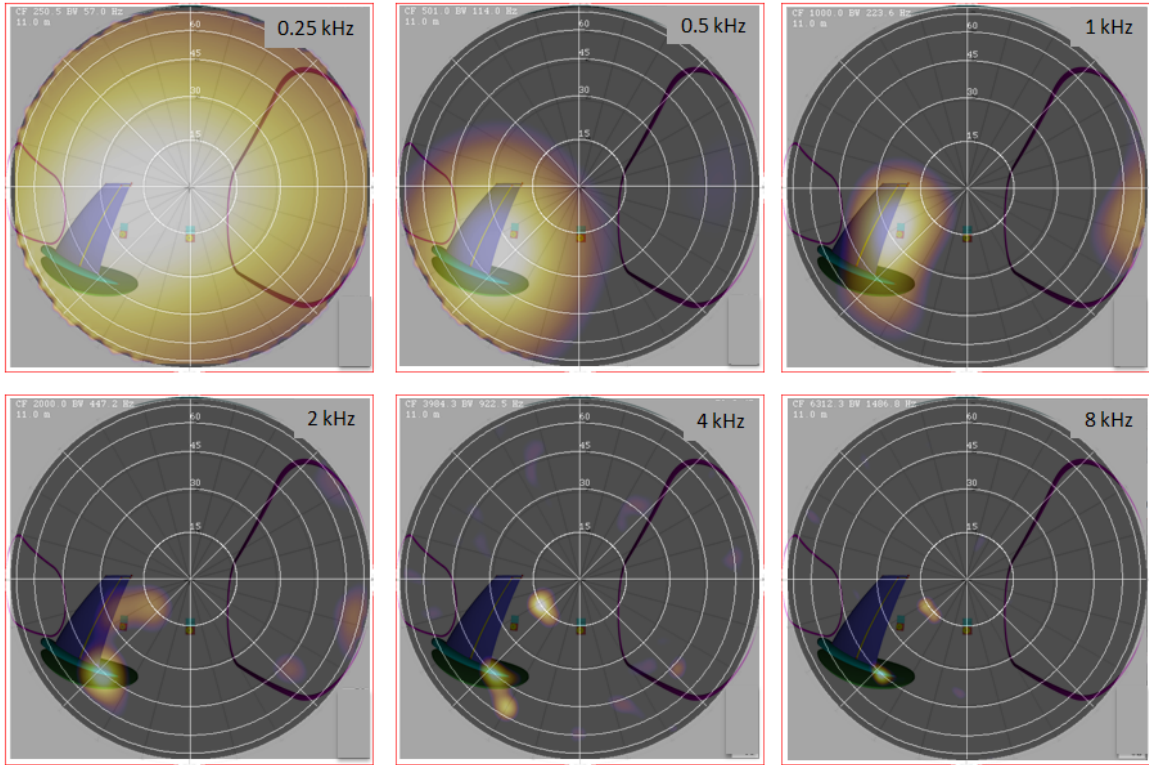


Fig 16. 757 active rudder non-actuated side beam form maps(B25 array), 100 kts, 6 actuators active.

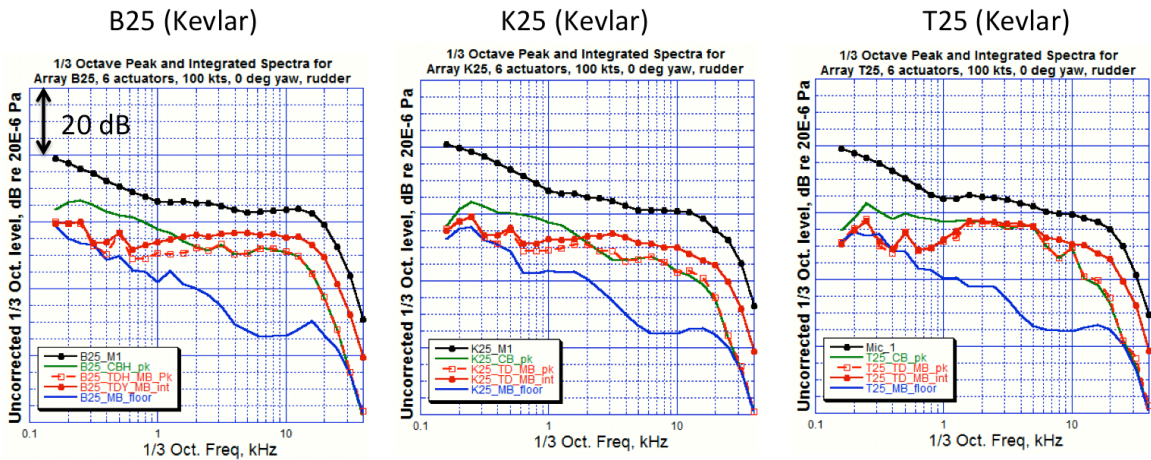


Fig. 17 757 active rudder non-actuated side sample spectra
 - black: microphone 1
 - blue: estimated peak array background noise level (background subtract)
 - green – conventional beamform peak (background subtract)
 - red open – TIDY process peak (background subtract)
 - red closed – TIDY process hemispheric integral (background subtract)

Appendix 1. Array microphone characteristics and locations

The microphones used for the wall mounted arrays were Countryman B3 electret lavalier microphones (model no. B3W5FF05CSR) with flat response (± 3 dB) from 20 to 20,000 Hz,. The same microphones were selected by Optinav for a 24 element array system (Array24jr) purchased previously for wind tunnel testing, and chosen for the high allowable pressure level range(24-150 dB). Before installation, the microphones were calibrated with a B&K 4228 pistonphone (250 Hz, 124 dB) as well as tested for quiescent noise averaging 25 dBA. Fig A1 is a histogram of the microphone sensitivities measured at room temperature (70° F). About 70% of the microphones had a sensitivity within ± 1 dB of the mean. A sample microphone was tested for temperature effect on sensitivity, which was found to be -0.036 dB/°C.

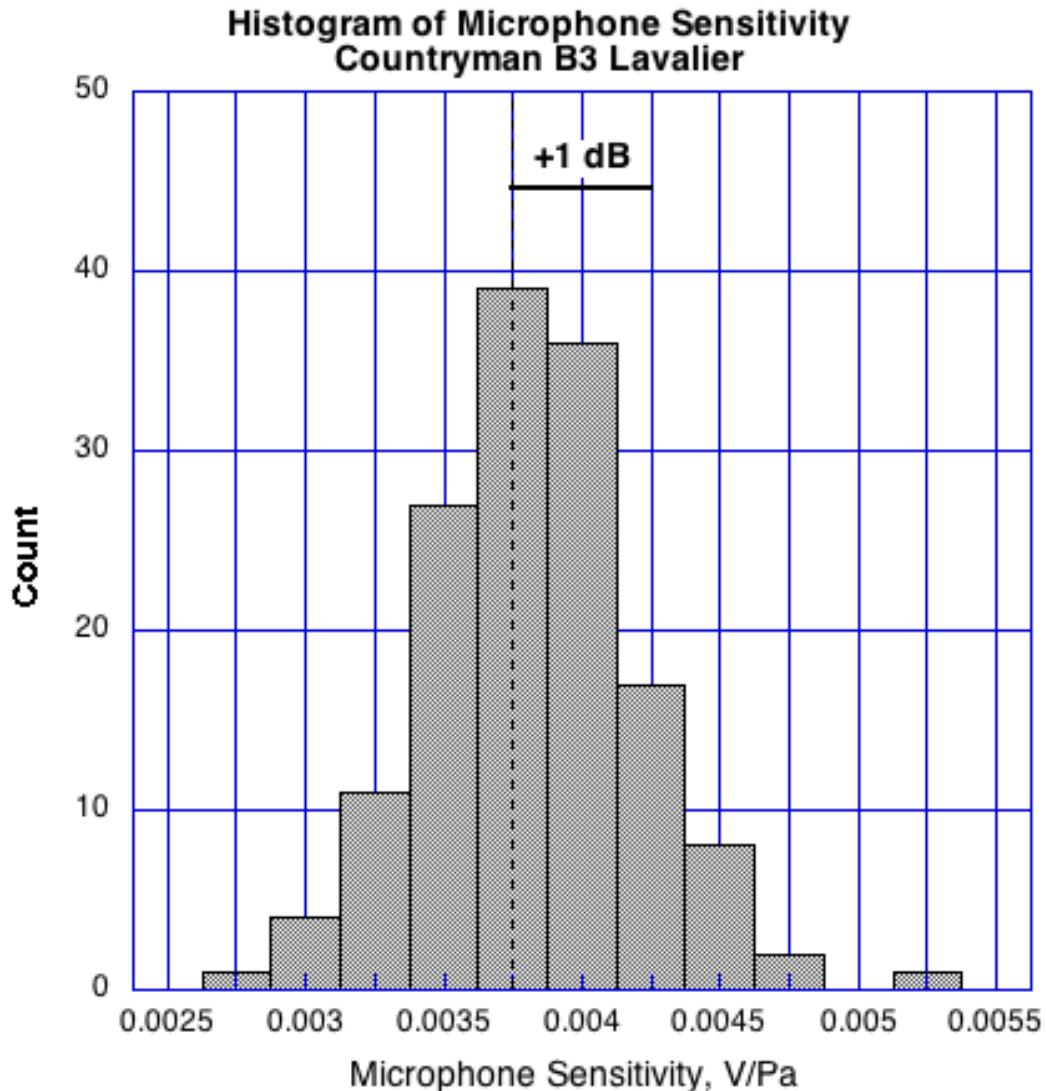


Fig. A1.1 Histogram of microphone sensitivities measured with B&K 4228 pistonphone. Countryman B3 electret, 24-150 dBA response range, 0.23"D x 0.18" long.

Mic #	X, in	Y, in	Mic #	X, in	Y, in
1	6.000	0.000	13	-4.360	-11.76
2	-3.000	5.200	14	12.36	2.100
3	-3.000	-5.200	15	-8.000	9.660
4	2.920	6.700	16	3.200	-13.48
5	-7.260	-0.8260	17	10.08	9.500
6	4.340	-5.860	18	-13.26	3.980
7	-8.220	4.520	19	9.960	-11.28
8	0.2040	-9.380	20	4.800	14.26
9	8.020	4.860	21	-14.74	-2.980
10	-9.820	-5.100	22	14.70	-6.700
11	9.340	-5.960	23	-1.558	16.08
12	0.4880	11.06	24	-13.14	-9.380

Table A1.2. Microphone locations for the base 24 element array.

Table A2 lists the microphone locations for the base 24 element array. The minimum microphone radius was 6 in. and the maximum radius just over 16 in. The x-coordinates were sign-reversed for the B2, K2, and T2 arrays. The y-coordinates were sign reversed for the B25, K25, and T25 arrays.

array	X, inches	Y, inches	Z, inches
B2	370.911	465.668	171.341
B25	370.911	-465.668	171.341
K2	-13.089	465.023	171.521
K25	-13.089	-465.023	171.521
T2	-349.089	464.459	171.682
T25	-349.089	-464.459	171.682

Table A1.3. Array locations in AEDC NFAC 40x80- Ft Wind Tunnel relative to the turntable center. X is measured downstream, Y to the right looking upstream, Z is towards the ceiling. The normal vector from the center of each array points 16.875° above the horizon. During the speaker calibration, the center speaker was located at X = -34.0, Y = 0.5, Z = 64.94 inches.

Appendix 2. Preamplifier design and connections to data acquisition system

Although power supply - preamplifiers are commercially available for the selected microphones, it was decided to use custom units designed and built by AerospaceComputing, Inc. to reduce module size and enable the use of low voltage DC rather than 120V AC power in the wind tunnel test section. Each array was provided with a 24 channel amplifier module positioned behind the array in the anechoic wedges of the 42" deep acoustic liner. The amplifier module included a regulated power source, coupling circuit, and line driver for each channel and was powered by a +/- 15V regulated tracking power supply located in the balance house under the turntable, that also housed the data acquisition system and control computers. The array amplifiers were connected to the data acquisition system with coaxial cable bundles 140-ft in length. The data acquisition computers were controlled remotely from the wind tunnel computer room with KVM extender switches.

The sensitivity of the microphones. 0.00375 V/Pa was such that the microphone output at maximum input of 150dBA would be 2.4 Vrms. No further amplification was needed for A/D converters with either +/- 5-10V range. A diagram of one of the amplifier/line-driver modules is shown below in Fig. A2.1

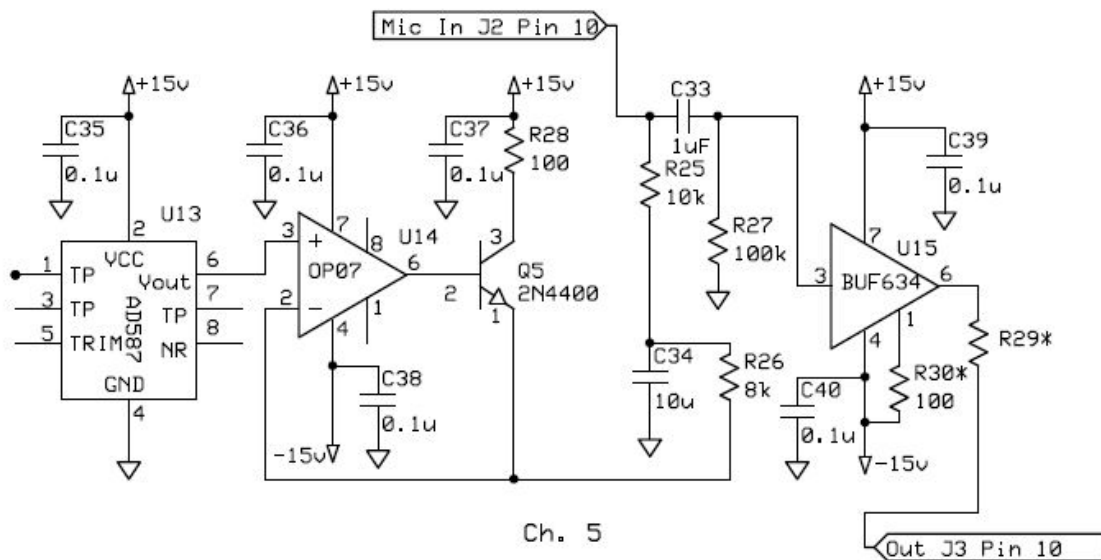


Fig A2.1 Circuit diagram of electret microphone power supply/line driver. The left-most circuit is a +10V precision voltage reference for microphone power. The right most circuit is the line driver capable to driving 1000 ft of RG174 with flat response to at least 100 kHz.

Each 24-channel unit consists of three 8-channel circuit board approximately 6 inches x 6 inches that are mounted in an enclosure approximately 10" W x 3.9" H x 9.6" D, as shown in Fig. A2.2 and described in reference below.



Fig. A2.2 Front(outputs) and back (microphone jacks) of 24 channel microphone interface module EM-2. Power supply connector is front lower right (+/- 15V).

Specification summary: microphone interface EM-2
 10 V ref. voltage generator: Analog Devices AD587
 Current booster amplifier: Analog Devices OP07
 Analog line drivers: Texas Instrument / Burr-Brow BUF634
 Amplifier bandwidth: > 30 MHz
 Low frequency cut-off (-3 dB) 1 Hz
 Amplitude response variation between channels (measured 0.01-100 kHz) < 0.1 dB
 Phase response variation between channels (measured 0.01-100 kHz) < 0.2 deg
 Microphone excitation voltage: 10.00 V
 Power input requirement +/- 15 V DC + common ground
 Quiescent current: 128 mA (EM-2)
 Environment: passive cooling only (no fans), device temp < 70°C

Reference.: Kumagai, H., "Electret Condenser Microphone Interface System for NASA/Ames Research Center Fluid Mechanics Lab 24-element Acoustic Arrays: Models EM-1 and EM-2", July 3, 2013. AerospaceComputing, Inc, 465 Fairchild Dr, Suite 224, Mountain View, CA 94043, (650) 988-0388